Current Dynamics during Disruptions in Large Tokamaks

L.-G. Eriksson,[1] P. Helander,[2] F. Andersson,[3] D. Anderson,[3] and M. Lisak[3]
[1]*Association EURATOM-CEA, CEA/DSM/DRFC, CEA-Cadarache, St. Paul lez Durance, France*
[2]*EURATOM/UKAEA Fusion Association, Culham Science Centre, Abingdon, United Kingdom*
[3]*Department of Electromagnetics, Chalmers University of Technology and EURATOM-VR Association, Göteborg, Sweden*
(Received 27 November 2003; published 19 May 2004)

Self-consistent modeling of the evolution of the plasma current during disruptions in large tokamaks is presented, taking into account both the generation of runaway electrons and their backreaction on the electric field. It is found that the current profile changes dramatically, so that the postdisruption current carried by runaway electrons is much more peaked than the thermal predisruption current. Although only a fraction of the thermal current is converted into runaway electrons, the central current density increases significantly for typical parameters in JET and ITER. It is also shown that the radial runaway profile can easily become filamented in the radial direction.

DOI: 10.1103/PhysRevLett.92.205004 PACS numbers: 52.55.Fa, 52.35.Py, 52.65.Pp

Tokamak discharges are frequently terminated by disruptions causing large mechanical and thermal loads on the vessel. Of particular concern is the generation of "runaway" electrons, which are accelerated to relativistic energies by the electric field induced during the thermal quench of the disruption. These electrons can damage the first wall on impact, and since the ease with which runaways are generated (in "avalanches," discussed below) increases exponentially with plasma current [1,2], this is an issue of prime importance for a next-step device such as ITER [3]. In this Letter, we present self-consistent modeling of runaway generation and current evolution during disruptions in large tokamaks, recognizing that the current carried by the runaway electrons modifies the electric field responsible for their own generation. The evolution of the current and the electric field must therefore be calculated self-consistently, which to our knowledge has not been accomplished before in kinetic runaway avalanche calculations. The result is interesting and surprising: it is found that the runaway current profile becomes very different from the predisruption current profile. In the past, it has usually been assumed that the current profile should not change much during a disruption in a tokamak like ITER, where avalanche runaway generation is very efficient [2,4,5]. In contrast, we find that the current density can increase substantially in the center of the discharge in both present and future devices, which could make the runaway beam more unstable and the postdisruption plasma more difficult to control.

The initial phase of a tokamak disruption is characterized by large-scale plasma instability, which causes the plasma to interact with the first wall. We do not consider this early stage of the disruption, but instead confine our attention to the thermal quench and subsequent evolution of the plasma. It is at this stage, when the plasma has regained axisymmetry, that most runaway electrons are believed to be generated. In the thermal quench, the plasma resistivity increases dramatically and a large toroidal electric field is induced that produces runaway electrons. There are two essentially different runaway generation mechanisms: primary (Dreicer) and secondary (avalanche) generation. The former is caused by a Fokker-Planck diffusion process in velocity space and generates runaways at the rate [6]

$$\dot{n}_r^I = \frac{n_e}{\tau}\left(\frac{m_e c^2}{2T_e}\right)^{3/2}\left(\frac{E_D}{E_\parallel}\right)^{3/8}\exp\left(-\frac{E_D}{4E_\parallel}-\sqrt{\frac{2E_D}{E_\parallel}}\right), \quad (1)$$

where $\tau = 4\pi\epsilon_0^2 m_e^2 c^3/n_e e^4 \ln\Lambda$ is the relativistic electron collision time [7,8], $E_\parallel$ the parallel electric field, and $E_D = m_e^2 c^3/e\tau T_e$ the Dreicer field. Secondary runaway production is caused by collisions at close range between existing runaway electrons and thermal ones and increases the density of the former at the rate [2]

$$\dot{n}_r^{II} \simeq \left(\frac{\pi}{2}\right)^{1/2}\frac{n_r(E_\parallel/E_c - 1)}{3\tau\ln\Lambda}, \quad (2)$$

in a pure plasma, where $E_c = m_e c/e\tau$ is the relativistic cutoff field below which no runaway generation can occur [8]. Since secondary generation causes exponential growth of the runaway population, this mechanism is frequently referred to as a runaway avalanche.

In the past, most of the theoretical effort devoted to runaway electrons has focused on the production mechanisms, e.g., on the derivation of the rates (1) and (2), but relatively little analysis has been performed on their consequences for integrated disruption modeling. A quantitative understanding of runaway generation in disruptions has largely been lacking. To address this issue, we have developed a new computational tool, the ARENA code, which solves the relativistic drift kinetic equation for electrons in toroidal geometry and calculates the electric field self-consistently. This code has recently been described in detail elsewhere [9]; here we give an account of the first systematic studies using ARENA. The code solves the kinetic equation as an initial-value problem through a Monte Carlo method, where the statistics of the high-energy tail of the distribution function is improved

by a weighting scheme that enhances the relative importance of the runaway region in velocity space. Crucially, the entire cross section of the plasma is simulated since this is necessary to calculate the evolution of the electric field. This is governed by the induction equation $\nabla \times \nabla \times \mathbf{E} = -\mu_0 \partial \mathbf{j}/\partial t$, which is solved by a finite element solver coupled to the Monte Carlo code. The current $\mathbf{j} = j_\parallel \mathbf{B}/B$ consists of two distinct parts: a thermal current equal to $\sigma_\parallel E_\parallel$, with $\sigma_\parallel$ the neoclassical conductivity, and the runaway current, which is obtained by integrating over the high-energy tail of the distribution function. Delicate problems of numerical stability arose in coupling the two codes but were solved by adopting a semi-implicit discretization of the problem, as detailed in Ref. [9]. As also described there, the code has been benchmarked extensively against previously published and novel analytical results, including Eqs. (1) and (2).

The thermal quench of a disruption and the subsequent evolution of the plasma current are simulated in ARENA by prescribing the evolution of the electron temperature as $T_e(r, t) = T_1(r) + [T_0(r) - T_1(r)]e^{-t/t_0}$, where $T_1 \ll T_0$. This causes the resistivity and the electric field to rise on the time scale t_0 (typically <1 ms) and leads to runaway electron generation, first by the primary mechanism and later by the secondary avalanche. Figure 1 shows an example of such a simulation, with parameters expected in ITER [10]. The initial plasma current was $I_p = 15$ MA, the density $n_e = 1.1 \times 10^{20}\ \mathrm{m}^{-3} \times (1 - 0.99x^2)^{0.1}$, the temperature evolved from $T_0 = 22$ keV $\times$ $(1 - 0.9x)$ to $T_1 = 5$ eV, $t_0 = 0.5$ ms, $x = r/a$ is the normalized radius and $a = 2.5$ m. In reality, this linear temperature profile, which is taken from Ref. [10], will probably be smoothed near the magnetic axis, but this does not affect the results significantly away from the axis. The rising runaway current limits the growth of the electric field at $t \simeq 4$ ms, which subsequently decays on a time scale set by the avalanche growth time and the skin time. At the end of the simulation, about two-thirds of the predisruption current has been replaced by runaways, mostly produced through avalanching. This is more than is usually observed in present day tokamaks and is due to the fact that the avalanche is much stronger in ITER. However, the most interesting result of the simulation is that the runaway current evolves to a profile that is more peaked than the predisruption current. Although only two-thirds of the initial current is converted to runaways, the current density on axis increases. As we shall see, this can be understood from the interplay between runaway generation and radial diffusion of the electric field.

Qualitatively similar results are obtained with parameters appropriate to JET. As already mentioned, avalanching is weaker than in ITER, but most runaways are still produced by the secondary mechanism. If the final temperature (which is not known experimentally) is chosen appropriately, the edge loop voltage, the time scale of runaway formation, and current conversion efficiency are all in rough agreement with experiment. Again, the current density on axis increases, typically by a factor of about 2. Interestingly, this may actually have been observed on JET, although it was not recognized at the time. In Ref. [5] the postdisruption runaway current profile was measured and the safety factor on axis was reported to be $q_0 \simeq 0.6$, suggesting a higher current density than before the disruption.

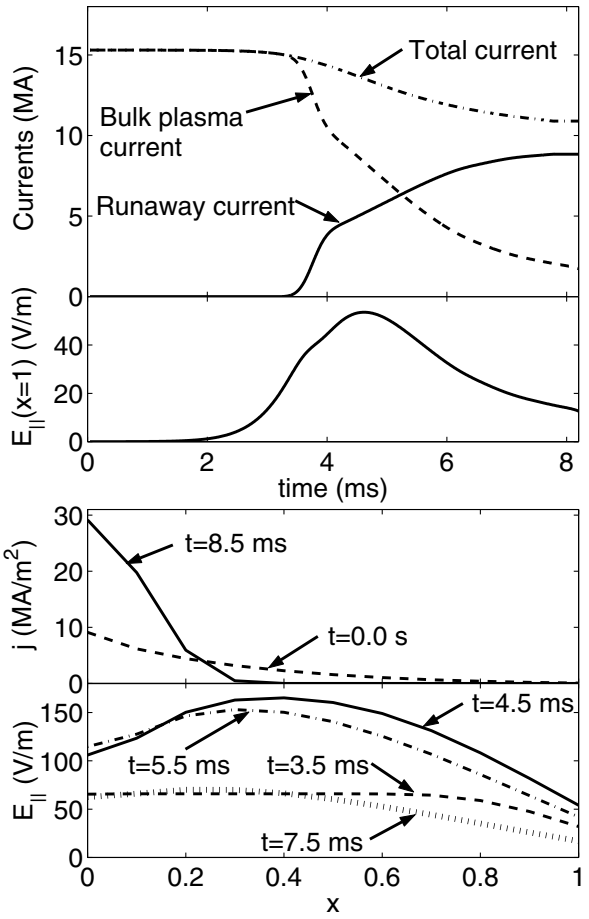

FIG. 1. ARENA simulation of the runaway dynamics in an ITER disruption.

It is possible to gain insight into the ARENA simulations from a reduced description of the plasma obtained by assuming that all runaways move at the speed of light, so that the current is $j_\parallel(x, t) = \sigma_\parallel(x, t)E_\parallel(x, t) + n_r(x, t)ec$. The runaway density n_r increases according to the sum of Eqs. (1) and (2), and the electric field is taken to evolve according to the induction equation in cylindrical geometry, $\nabla^2 E_\parallel = \mu_0 \partial j_\parallel/\partial t$. Writing $n = n_r/n_{r0}$, where $n_{r0} = j_0/ec$ and j_0 is the predisruption current density on axis, $E = E_\parallel/E_c(0)$, and normalizing time to $3(2/\pi)^{1/2}\tau_0 \ln\Lambda$, with $\tau_0 = \tau(x = 0)$, then gives the following system of coupled differential equations,

$$\partial_t n = F(E) + nE, \tag{3}$$

$$\partial_t(\sigma E + n) = \alpha^{-1}\hat{\nabla}^2 E, \tag{4}$$

where we have assumed $E \gg 1$ and written $\hat{\nabla}^2(\cdots) =$

$x^{-1}\partial_x[x\partial_x(\cdots)]$, $\sigma(x,t) = m_e\sigma_\parallel/n_{r0}e^2\tau_0$,

$$F(E,x,t) = \frac{3\ln\Lambda n_e(0)\hat{n}^{19/8}}{2\pi^{1/2}n_{r0}u^{15/4}E^{3/8}}e^{-(1/4u^2E)-\sqrt{2/u^2E}},$$

$$\alpha = \frac{(2\pi)^{3/2}}{3\ln\Lambda}\frac{j_0a^2}{I_A},$$

with $u^2(x,t) = T_e(x,t)/m_ec^2 \ll 1$, $\hat{n} = n_e(x)/n_e(0)$, and $I_A = 4\pi m_ec/\mu_0e$ the Alfvén current. Equations (3) and (4) govern the evolution of the normalized runaway current density $n(x,t)$ and electric field $E(x,t)$, if $T_e(x,t)$ and hence $\sigma(x,t)$ are given. The boundary condition on the electric field is $E(1,t) = 0$ if the plasma is surrounded by a perfectly conducting wall at $x = 1$. If the wall is instead at $x = b > 1$, with a vacuum region in the region $1 < x < b$, then the boundary condition at $x = 1$ is obtained by matching to the vacuum solution $E(x,t) \sim \ln(b/x)$, giving $E(1,t) + (\ln b)\partial_xE(1,t) = 0$.

The parameter α is closely related to the usual estimate for the number of exponentiations in the avalanche $I_p/I_A\ln\Lambda$ [2], which is a large number in ITER. In the limit $\alpha \to \infty$, the left-hand side of (4) must vanish. Diffusion of the electric field is then negligible and the current density cannot change: $n + \sigma E$ is constant at each radius. It is "infinitely easy" to generate secondary runaways in this limit, and the conversion of thermal current into runaways is perfect. This is effectively the case considered in previous works [2,4,5] on grounds that $\alpha \sim O(10^2)$ or higher in ITER and JET.

However, if α is allowed to be finite, new and important phenomena emerge since this allows current to diffuse radially. Figure 2 shows an example where Eqs. (3) and (4) were solved with parameters chosen to match a recent JET disruption experiment. The results are very similar to both the corresponding ARENA simulation (not shown) and to experiment: the current conversion efficiency is about a half, the time scale is a few ms, and the current density increases on axis. According to Eq. (4) radial diffusion of the electric field occurs when $\alpha \neq \infty$, and this leads to two phenomena seen in both Figs. 1 and 2. First, because some electric field is lost to the boundary and is not available to generate runaways, the current conversion efficiency is lower than if $\alpha \to \infty$. Second, because of the exponential sensitivity of the function F to the electron temperature, most runaways are initially produced close to the magnetic axis. The electric field is then reduced there so that its radial profile becomes hollow and $E(x,t)$ has a local minimum on axis, as seen in the last panel of Fig. 1. This makes more electric field diffuse into the center, leading to enhanced runaway production there at the expense of less generation elsewhere. This mechanism, which is much stronger than that caused by toroidal effects [11], is what causes the peaking of the runaway current in our simulations.

An analytical understanding of these processes can be gained by noting that primary generation is very swift,

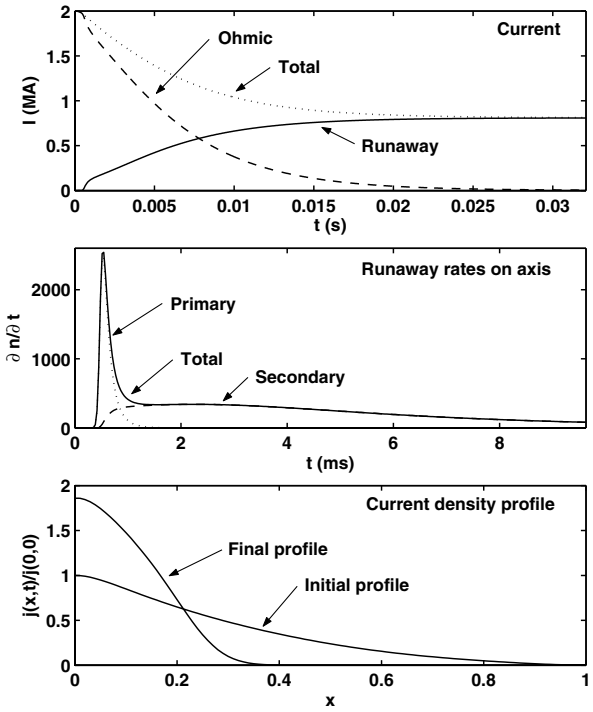

FIG. 2. Numerical solution of Eqs. (3) and (4) for JET parameters, $I_p = 2$ MA, $n_e = 5\times10^{19}\ \mathrm{m}^{-3}\times(1-0.9x^2)^{1/2}$, $T_0 = 1.4\ \mathrm{keV}\times(1-0.9x^2)^2$, $T_1 = 10$ eV, $t_0 = 0.1$ ms

see Fig. 2, and occurs on a shorter time scale than the avalanche, which generates most of the runaways. After a short time, t_*, most subsequent runaway production will occur by the secondary mechanism and F can be neglected in Eq. (3). Eliminating $E = \partial_t\ln n$ from Eq. (4) and integrating with respect to time then gives

$$\sigma\partial_tN = j_* - e^N - \alpha^{-1}\hat{\nabla}^2(N_* - N),$$

where $N(x,t) = \ln n(x,t)$, $N_*(x) = \ln n(x,t_*)$ and $j_*(x) = \sigma(x,t_*)E(x,t_*) + n(x,t_*)$ is the total current at $t = t_*$. From this nonlinear partial differential equation for the runaway density an *ordinary* differential equation for the final state $N(x,\infty)$ follows by setting $\partial_tN = 0$,

$$e^N = j_* - \alpha^{-1}\hat{\nabla}^2(N_* - N). \tag{5}$$

This equation allows the final runaway current profile to be determined if the runaway "seed" from primary generation, $N_*(x)$, and the total current profile $j_*(x)$ at $t = t_*$ are known. Since the time t_* occurs very early, j_* is approximately equal to the initial current profile.

Although Eq. (5) appears difficult to solve in general, a number of important results can be deduced directly from this equation. First, it can be shown that the final current is always smaller than the initial current, i.e., regardless of its radial profile the runaway current can never exceed the predisruption current, as always observed in experiments. Second, it follows from Eq. (5) that fine-scale variations in the seed current are "inherited" by the final current. Since the highest

derivative operates on $N - N_*$, this difference cannot vary suddenly. For instance, if N_* jumps by an amount y at the location x, so that $N_*(x+) - N_*(x-) = y$, then N jumps by the same amount, $N(x+) - N(x-) = y$, implying $n(x+)/n(x-) = e^y$. This may explain why the runaway current profile usually appears to have such an uneven radial structure in experiments [12] that x rays are emitted in a series of sharp bursts when the runaway beam eventually hits the wall. Primary generation is exceedingly sensitive to the electron temperature, so if one flux surface cools down more quickly than neighboring ones, e.g., as a result of thermal instability, then far fewer primary runaways are generated on this surface than on its neighbors. Although most runaways are generated by the secondary mechanism, the relative deficit of runaways remains throughout the duration of the avalanche if the spatial variation is of sufficiently fine scale, $\Delta x \lesssim \alpha^{-1/2}$. Figure 3 shows a dramatic illustration of this effect. Here, Eqs. (3) and (4) are solved with the same parameters as in Fig. 2, but the cooling time t_0 is taken to have a small, fine-scale radial variation, $t_0 = 0.1\ \mathrm{ms} \times [1 + 0.1 \sin(40\pi x)]$. This does not affect the overall conversion efficiency from Ohmic current to runaway current, but the latter acquires huge radial variations.

A third consequence of Eq. (5) is that the final current profile will tend to be peaked around $x = 0$ if this is true for the seed profile N_*. The latter can be calculated approximately by assuming that (i) diffusion is negligible on the fast time t_*, so that $j(x) = \sigma E + n$ is independent of time for $t < t_*$; (ii) the seed from primary generation is small, $e^{N_*} \ll 1$; and (iii) the thermal quench is very fast, so that the conductivity falls instantly from its predisruption value to a small value $\sigma_1(x)$. These three assumptions are fairly well satisfied in JET, and imply that the electric field just after the thermal quench is $E_1(x) = j(x)/\sigma_1(x) \gg 1$. It follows from Eq. (3) that the electric field $E_*(x)$ at the time t_* when secondary runaway generation overtakes primary generation is determined by $F(E_*) = (j - \sigma_1 E_*)E_*$, and satisfies $E_* \simeq E_1$. Hence the runaway seed profile becomes $n_* = e^{N_*} = F(E_*)/E_*$ and

$$\hat{\nabla}^2 N_* \simeq -\hat{\nabla}^2 (E_D/4E_\parallel + \sqrt{2E_D/E_\parallel}),$$

with E_D and $E_\parallel = E_c(0)E_1$ measured just after the thermal quench. This result agrees very well with the full numerical solution of Eqs. (3) and (4). Since $E_D/E_\parallel \gg 1$ and the temperature is normally more peaked than the density in the center of the plasma, $(\hat{\nabla}^2 n_e)/n_e \lesssim (\hat{\nabla}^2 T_e)/T_e$, this implies a peaked seed profile $-\hat{\nabla}^2 N_* \gg 1$. In fact, for typical parameters $-\hat{\nabla}^2 N_*$ is as large as α, so that Eq. (5) predicts strong current peaking although $\alpha \gg 1$.

In summary, numerical simulation and analytical modeling have allowed a quantitative understanding to be gained of runaway electron production during tokamak disruptions. The results suggest that the current profile should change dramatically when Ohmic current is converted to runaway electrons. The runaway current profile is likely to become filamented in the radial direction, and for typical JET and ITER parameters the current channel is predicted to narrow considerably and the axis current density to increase. This could make the postdisruption plasma less stable, in particular, if the central safety factor q_0 falls far below unity.

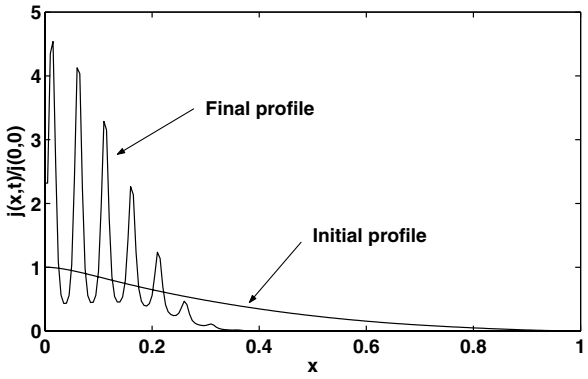

FIG. 3. Current profiles in a simulation similar to Fig. 2, but with the cooling time t_0 varying sinusoidally by 10%.

This work was funded jointly by EURATOM and the U.K. Engineering and Physical Sciences Research Council.

[1] R. Jayakumar, H. H. Fleischmann, and S. Zweben, Phys. Lett. A **172**, 447 (1993).
[2] M. N. Rosenbluth and S.V. Putvinski, Nucl. Fusion **37**, 1355 (1997).
[3] Special issue on ITER Physics Basis, edited by F.W. Perkins *et al.* [Nucl. Fusion **39**, 2137 (1999)].
[4] R.W. Harvey, V. S. Chan, S. C. Chiu, T. E. Evans, M. N. Rosenbluth, and D. G. Whyte, Phys. Plasmas **7**, 4590 (2000).
[5] R. D. Gill, B. Alper, A.W. Edwards, L. C. Ingesson, M. F. Johnson, and D. J. Ward, Nucl. Fusion **40**, 163 (2000).
[6] A.V. Gurevich, Sov. Phys. JETP **12**, 904 (1961); M. D. Kruskal and I. B. Bernstein, Princeton Plasma Physics Laboratory Report No. MATT-Q-20, 1962, p. 174; R. H. Cohen, Phys. Fluids **19**, 239 (1976).
[7] P. Helander and D. J. Sigmar, *Collisional Transport in Magnetized Plasmas* (Cambridge University, Cambridge, England, 2002).
[8] J.W. Connor and R. J. Hastie, Nucl. Fusion **15**, 415 (1975).
[9] L.-G. Eriksson and P. Helander, Comput. Phys. Commun. **154**, 175 (2003).
[10] *Summary of the ITER Final Design Report* (IAEA, Vienna, 2001).
[11] M. Schittenhelm, in *Proceedings of the 24th European Physical Society Conference on Plasma Physics and Controlled Fusion, Berchtesgaden, 1997* (European Physical Society, Geneva, 1997), Vol. III, p. 985.
[12] R. D. Gill, Nucl. Fusion **33**, 1613 (1993).